Inorganic Chemistry

Article

pubs.acs.org/IC

Enneanuclear $[Ni_6Ln_3]$ Cages: $[Ln^{III}_3]$ Triangles Capping $[Ni^{II}_6]$ Trigonal Prisms Including a $[Ni_6Dy_3]$ Single-Molecule Magnet

Angelos B. Canaj,[†] Demetrios I. Tzimopoulos,[‡] Milosz Siczek,[§] Tadeusz Lis,[§] Ross Inglis,*[,∥] and Constantinos J. Milios*[,†]

[†]Department of Chemistry, The University of Crete, Voutes, 71003, Herakleion, Greece

[‡]Department of Chemistry, Aristotle University of Thessaloniki, 54124 Thessaloniki, Greece

[§]Faculty of Chemistry, University of Wroclaw, Joliot-Curie 14, 50-383, Wroclaw, Poland

[∥]School of Chemistry, The University of Edinburgh, David Brewster Road, EH9 3FJ Edinburgh, U.K.

Supporting Information

ABSTRACT: The use of (2-(β-naphthalideneamino)-2-hydroxymethyl-1-propanol) ligand, H_3L, in Ni/Ln chemistry has led to the isolation of three new isostructural $[Ni^{II}_6Ln^{III}_3]$ metallic cages. More specifically, the reaction of $Ni(ClO_4)_2{\cdot}6H_2O$, the corresponding lanthanide nitrate salt, and H_3L in MeCN, under solvothermal conditions in the presence of NEt_3, led to the isolation of three complexes with the formulas $[Ni_6Gd_3(OH)_6(HL)_6(NO_3)_3]{\cdot}5.75MeCN{\cdot}2Et_2O{\cdot}1.5H_2O$ (**1**·5.75MeCN·$2Et_2O{\cdot}1.5H_2O$), $[Ni_6Dy_3(OH)_6(HL)_6(NO_3)_3]{\cdot}2MeCN{\cdot}2.7Et_2O{\cdot}2.4H_2O$ (**2**·2MeCN·$2.7Et_2O{\cdot}2.4H_2O$), and $[Ni_6Er_3(OH)_6(HL)_6(NO_3)_3]{\cdot}5.75MeCN{\cdot}2Et_2O{\cdot}1.5H_2O$ (**3**·$5.75MeCN{\cdot}2Et_2O{\cdot}1.5H_2O$). The structure of all three clusters describes a $[Ln^{III}_3]$ triangle capping a $[Ni^{II}_6]$ trigonal prism. Direct current magnetic susceptibility studies in the 5−300 K range for complexes **1**−**3** reveal the different nature of the magnetic interactions within the clusters: dominant antiferromagnetic exchange interactions for the Dy^{III} and Er^{III} analogues and dominant ferromagnetic interactions for the Gd^{III} example. Alternating current magnetic susceptibility measurements under zero external dc field displayed fully formed temperature- and frequency-dependent out-of-phase peaks for the $[Ni^{II}_6Dy^{III}_3]$ analogue, establishing its single molecule magnetism behavior with U_{eff} = 24 K.

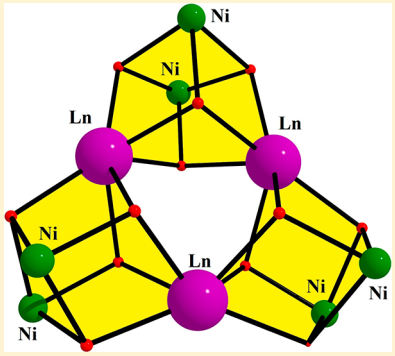

INTRODUCTION

One of the most active areas in the field of molecular magnetism is the search for single molecule magnets (SMMs), i.e., molecules that retain their magnetization once magnetized in the absence of magnetic field.[1] The number of such species has grown exponentially over the last 2 decades, with the phenomenon initially observed for transition-metal centers such as Mn, Fe, Co, and Ni, with the $[Mn_{12}OAc]$ and the $[Fe_8/tacn]$ molecules being the very first examples.[2] In addition, in 2003 the mononuclear complex $(NBu_2)[Pc_2Ln]$ (Ln = Tb, Dy) was also found to display SMM behavior, thus opening the way for 4f SMMs.[3] Nowadays, the introduction of 4f centers in the field of SMMs is mainly due to the two fundamental properties of lanthanides—(1) their large magnetic moment, since they can host up to seven unpaired electrons in the 4f orbitals, and (2) their large magnetic anisotropy, due to the large spin−orbit coupling present (with the exceptions of La^{III}, Gd^{III}, and Lu^{III})—both of which are the main prerequisites for the appearance of SMM behavior. Today, molecules with impressive SMM properties have been reported with examples including 4f centers, while the 3d SMMs seem to have reached their peak. These new 4f-containing species, either 3d−4f or purely 4f, display extremely large energy barriers for the reorientation of the magnetization, assuming, of course, that an Arrhenius analysis is valid for such systems.[4]

We recently reported the use of the naphthalene-based triol ligand H_3L [L = 2-(β-naphthalideneamino)-2-hydroxymethyl-1-propanol, Scheme 1] for the synthesis of polynuclear 3d complexes[5] and Mn-4f complexes.[6] Herein, we report the use

Scheme 1. Structure of the Ligand Discussed in the Text and Its Coordination Modes in 1−3

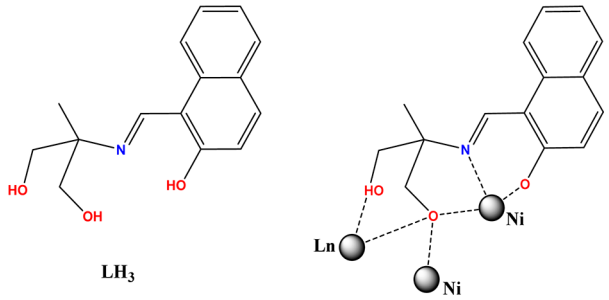

Received: May 21, 2015
Published: July 2, 2015

DOI: 10.1021/acs.inorgchem.5b01149
Inorg. Chem. 2015, 54, 7089−7095

of this triol Schiff base ligand for the synthesis of a new family of enneanuclear $[Ni^{II}_6Ln^{III}_3]$ complexes.

EXPERIMENTAL SECTION

All manipulations were performed under aerobic conditions, using materials as received (reagent grade). ***Caution!*** *Although no problems were encountered in this work, care should be taken when using the potentially explosive perchlorate anions.* H_3L was synthesized by the reaction of 2-hydroxy-1-naphthaldehyde with 2-amino-2-methyl-1,3-propanediol in MeOH, as described in the literature.[7] Elemental analyses (C, H, N) were performed by the University of Ioannina microanalysis service. Variable-temperature, solid-state, direct current (dc) magnetic susceptibility data down to 5 K were collected on a Quantum Design MPMS-XL SQUID magnetometer equipped with a 7 T dc magnet at the University of Edinburgh. Diamagnetic corrections were applied to the observed paramagnetic susceptibilities using Pascal's constants. EDS measurements were performed on a JEOL JSM-6390LV scanning electron microscope at the University of Crete.

General Synthetic Procedure for Complexes 1−3. All three complexes were prepared from the reaction between $Ni(ClO_4)_2·6H_2O$ (110 mg, 0.3 mmol), the corresponding $Ln(NO_3)_3·6H_2O$ salt (0.3 mmol), and H_3L (78 mg, 0.3 mmol) in the presence of excess base, NEt_3, in MeCN under solvothermal conditions (95 °C, 20 h). After cooling to room temperature, the resulting green solution was layered with Et_2O (10 mL), and green crystals of the general formulas $[Ni_6Ln_3(OH)_6(HL)_6(NO_3)_3]·5.75MeCN·2Et_2O·1.5H_2O$ were isolated in ∼35−45% yields after ∼3 days (Ln = Gd, **1**·5.75MeCN·2Et_2O·1.5H_2O; Er, **3**· 5.75MeCN·2Et_2O·1.5H_2O). For the Dy analogue, the formula was found to be $[Ni_6Dy_3(OH)_6(HL)_6(NO_3)_3]·2MeCN·2.7Et_2O·2.4H_2O$ (**2**·2MeCN·2.7Et_2O·2.4H_2O).

Anal. Calcd (found) for **1**·2MeCN·1H_2O: C 40.73 (40.57), H 3.78 (3.50), N 5.56 (5.51); **2**·1MeCN·1H_2O: C 40.23 (40.37), H 3.71 (3.43), N 5.10 (4.96); **3**·2MeCN·1H_2O: C 40.30 (40.43), H 3.74 (3.48), N 5.50 (5.65).

X-ray Crystallography. Diffraction data for **1**·5.75MeCN·2Et_2O·1.5H_2O, **2**·2MeCN·2.7Et_2O·2.4H_2O, and **3**·5.75MeCN·2Et_2O·1.5H_2O were collected at 80 K on a Xcalibur R four-circle diffractometer with a ruby CCD detector. The structure of **3** was solved by direct methods with SHELXS. The structures of **1**−**3** were refined by full-matrix least-squares techniques on F^2 with SHELXL.[25] The refinement of the structures for **1** and **2** was started by using the coordinates of the heavy atoms taken from the isomorphous crystal **3**. The H atoms were included in an idealized geometry riding on their parent atoms with C−H = 0.95−0.99 Å and with $U_{iso}(H) = 1.2U_{eq}(CH,CH_2)$ or $1.5U_{eq}(CH_3)$, except for water H atoms, which were located in the Fourier maps and refined with O−H distances restrained to 0.840(1) Å and then parent atoms were constrained (AFIX 3 instruction). Data collection parameters and structures solution and refinement details for structures **2** and **3** are listed in Table S1 (Supporting Information). Crystals of compound **1** decompose during measurements between room temperature and 240 K and show slight twinning during decreasing of the temperature to 80 K. Preliminary refinement, on data from twinned crystal, had been made and showed that the structure is isomorphous with crystal **3**. Unfortunately, high residual peaks around heavy atoms (Gd and Ni) had been observed, and for this reason, as well as the high R factor (≈0.17), these results are not of good quality.

RESULTS AND DISCUSSION

Synthesis. The formation of complexes **1**−**3** occurred upon the reaction of $Ln(NO_3)_3·6H_2O$ (Ln = Gd, Dy, Er), $Ni(ClO_4)_2·6H_2O$, and H_3L in 1:1:1 ratio in the presence of an excess of NEt_3 in MeCN, under high-pressure and high-temperature conditions, according to eq1:

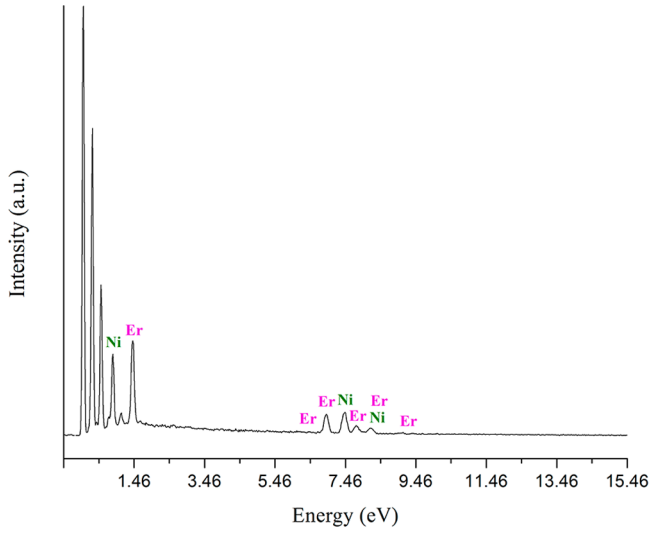

Figure 1. EDS analysis of complex **3**.

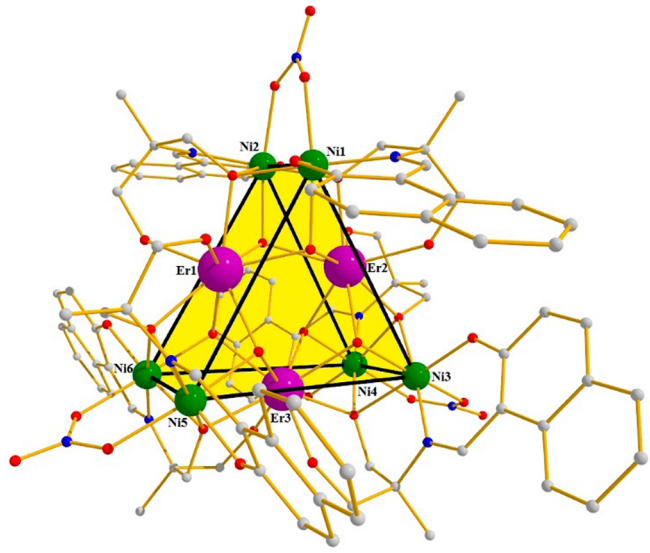

Figure 2. Molecular structure of **3**. Solvent molecules and H atoms are omitted for clarity. Color code: Ni = green, Er = purple, O = red, N = blue, and C = gray.

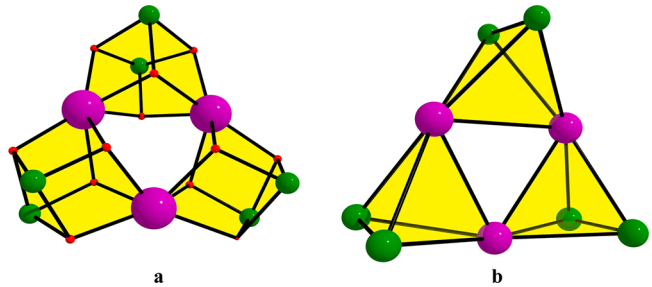

Figure 3. Metallic core of complexes **1**−**3** described as (a) corner-sharing $[Ni_2Ln_2(HL)_2(OH)_2]$ cubanes and (b) corner-sharing $[Ni_2Ln_2]$ tetrahedra. Color code: Ni = green, Ln = purple, and O = red.

$$6Ni(ClO_4)_2·6H_2O + 3Ln(NO_3)_3·6H_2O + 6H_3L + 6OH^- \xrightarrow{MeCN} [Ni_6Ln_3(OH)_6(HL)_6(NO_3)_3] + 12ClO_4^- + 6NO_3^- + 12H^+ + 54H_2O \quad (1)$$

DOI: 10.1021/acs.inorgchem.5b01149
Inorg. Chem. 2015, 54, 7089−7095

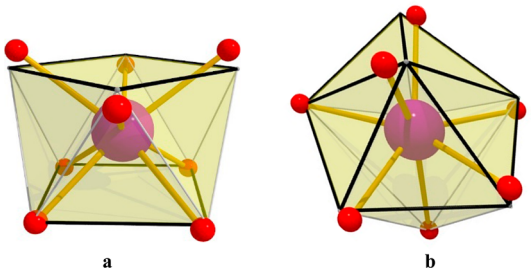

Figure 4. (a) Square antiprismatic coordination sphere for Er(1) and (b) triangular dodecahedron for both Er(2) and Er(3), as calculated with the program SHAPE.

In order to investigate how the reaction's conditions affect the identity of the products, we tried changing the amount/nature of the base used, as well as the time of the reaction. By repeating the reaction in the absence of base, we were not able to isolate any crystalline material; as expected, the presence of base is crucial for the formation of the products, since besides deprotonating the six H_3L ligands it also provides the six μ_3-OH^- groups present in the structure (vide infra). In addition, despite the fact that we used an excess of base, the ligands were not fully deprotonated, since all six ligands were found to be in the doubly deprotonated HL^{2-} form. Furthermore, the nature of the base used (NEt_3, NMe_4OH, and NaOH) did not change the identity of the products, as verified by IR spectroscopy and X-ray powder diffraction. Finally, repeating the reaction under normal laboratory bench conditions did not lead to any crystalline material, thus showing the need for high temperature and pressure for the formation of **1**−**3**. For all three clusters we obtained large, single crystals suitable for X-ray single-crystal crystallography. In addition, we performed energy dispersive X-ray spectroscopy (EDS) measurements, a powerful tool that allows us to check the homogeneity of our crystals, in order to investigate the purity of the bulk crystalline material of **3** (Figure 1); the Ni:Er ratio was found to be 64.9:35.1, in excellent agreement with the theoretical value of 66.6:33.3 as established by single-crystal X-ray crystallography

Description of Structures. Selected interatomic distances and angles for clusters **2** and **3** are listed in Tables S2 and S3 (Supporting Information). Complexes **1** and **3** are isostructural, while complex **2** differs only in the number of the cocrystallized solvate molecules ($2MeCN{\cdot}2.7Et_2O{\cdot}2.4H_2O$ for **2** vs $5.75MeCN{\cdot}2Et_2O{\cdot}1.5H_2O$ for **1** and **3**); therefore, we will only provide a description of the $[Ni_6Er_3(OH)_6(HL)_6(NO3)_3]$

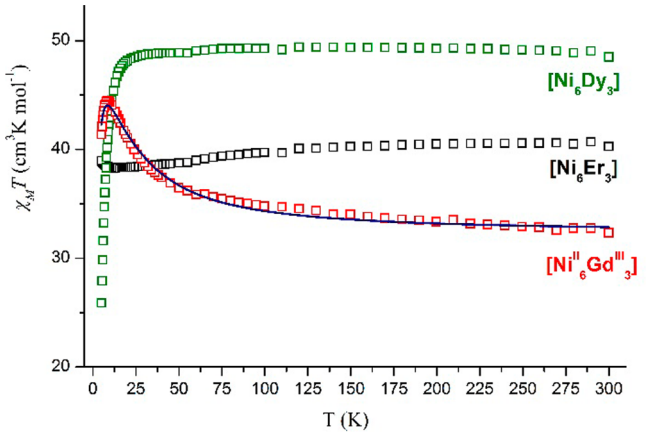

Figure 6. $\chi_M T$ vs T plot for complexes **1** ($[Ni_6Gd_3]$), **2** ($[Ni_6Dy_2]$), and **3** ($[Ni_6Er_3]$) under an applied dc field of 0.1 T. The solid line represents a fit of the data in the 5−300 K range (see the text for details).

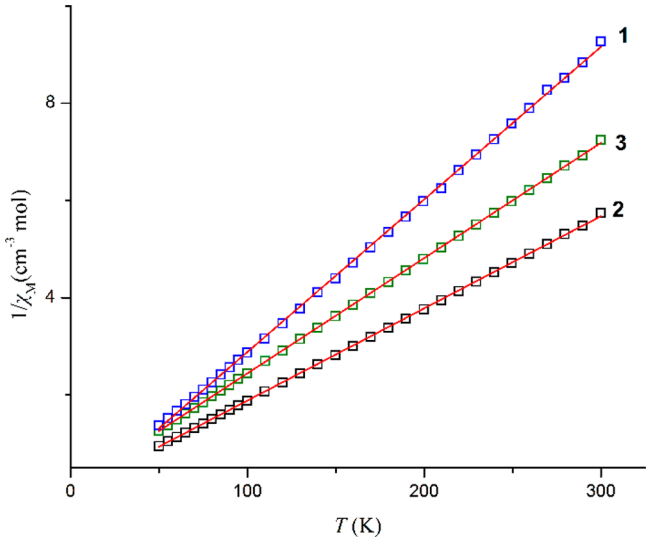

Figure 7. Curie−Weiss plot for complexes **1**−**3** for the 50−300 K range.

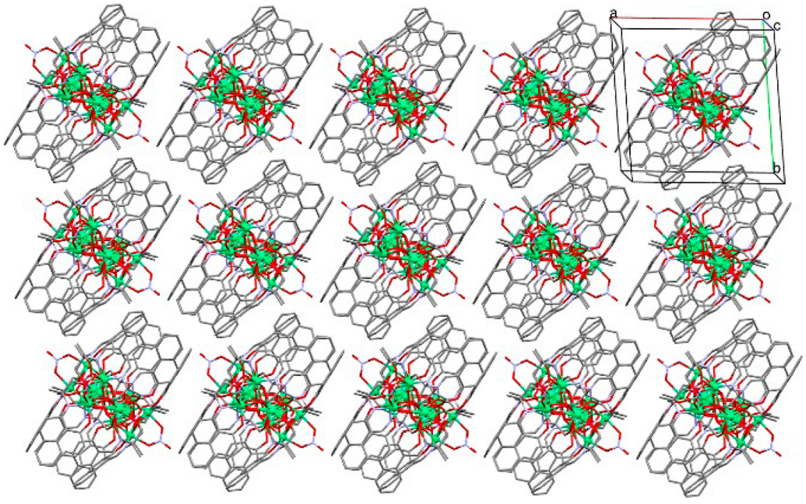

Figure 5. Crystal-packing of **3**.

DOI: 10.1021/acs.inorgchem.5b01149
Inorg. Chem. 2015, 54, 7089−7095

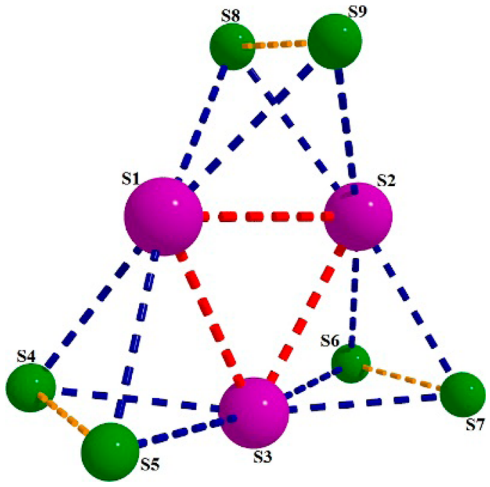

Figure 8. Exchange interaction scheme for **1**. Color code: red line = J_1, blue line = J_2, orange line = J_3; Gd = purple spheres and Ni = green spheres.

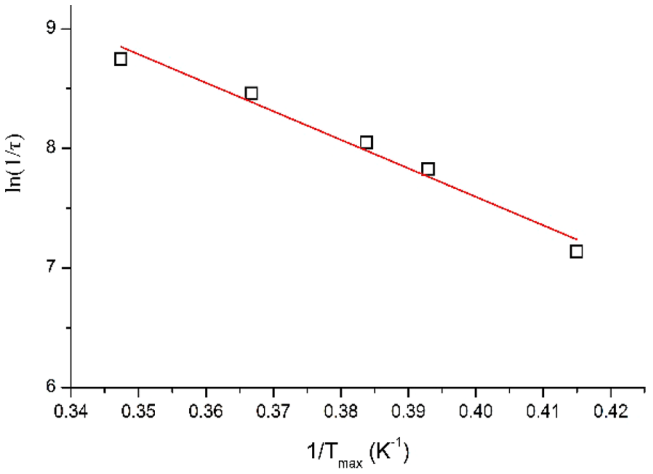

Figure 10. Arrhenius plot using powder ac magnetic susceptibility data for complex **2**.

complex (Figure 2) and highlight any differences between them and complex **2**; complex **3** crystallizes in the triclinic space group $P\bar{1}$; its metallic core consists of a $[Er_3^{III}]$ equilateral triangle (Er···Er = 3.6 Å) capping a $[Ni_6^{II}]$ trigonal prism. The lanthanide triangle is held in position by six μ_3-OH groups, with each one bridging two Er^{III} ions and one Ni^{II} ion. The $[Ni_6^{II}]$ trigonal prism consists of six μ_3-O_R alkoxide groups, belonging to the six doubly deprotonated 3.3111 (Harris notation)[8] HL^{2-} ligands, and three $\eta^1{:}\eta^1{:}\mu$ nitrate groups responsible for bridging the three $[Ni_2]$ pairs located at the corners of the trigonal prism. The depth of the prism is ∼2.84 Å, while its edge is ∼6.4 Å. All six HL^{2-}ligands adopt the same 3.3111 coordination mode. Alternatively, the metallic core may be envisaged as three corner-sharing $[Ni_2Er_2]$ tetrahedra or, finally, as three corner-sharing $[Ni_2Er_2(HL)_2(OH)_2]$ cubanes (Figure 3). All Ni^{II} centers have an O_5N coordination sphere adopting an octahedral geometry, while the three Er^{III} ions are eight-coordinate with their coordination sphere being exclusively oxygen dominated. Following a SHAPE analysis,[9] the theoretical polyhedra for the lanthanide centers were found to be square antiprismatic for Er(1) and triangular dodecahedron for both Er(2) and Er(3) (Figure 4). The Ni···O, Ni···N, and Ln···O bond lengths are ∼1.990−2.171, ∼1.978−1.980, and ∼2.29−2.36 Å, respectively, while the Ni···O···Ni, Ln···O···Ln, and Ni···O···Ln angles are in the ∼86.10°−86.60°, 102.10°−103.46°, and 104.55°−106.28° range, respectively.

In the crystal lattice there are no intermolecular H-bonds between the clusters, while the molecules of **1** and **3** form sheets of "tubes" in a head-to-tail fashion (Figure 5). Similarly, complex **2** adopts the same crystal packing as **1** and **3**, while again no intermolecular H-bonds are present. Complexes **1**−**3** join only a small family of structurally characterized $[M_6Ln_3]$ (M = Cu, Fe, Mn, Ni) cages of which there are only four examples: (i) complex $[Cu_6Dy_3L_6]$ (LH_2 = 1,1,1-trifluoro-7-hydroxy-4-methyl-5-aza-hept-3-en-2-one) with a trigonal prismatic structure,[10] (ii) cluster $[Fe_6Dy_3(\mu_4\text{-tea})_2(\mu_3\text{-teaH})_4]$ (H_3tea = triethanolamine) with a conelike structure,[11] (iii) complexes $[Mn_6Ln_3(L)_6]$ [HL= (*S*,*E*)-4-(2-hydroxybenzylideneamino)-2-hydroxybutanoic acid] (Ln = Dy, Tb, Gd),[12] and (iv) cluster $[Ni_6La_3(IDA)_6)]$ (IDA = iminodiacetate) with a hexagonal cagelike cluster.[13]

Finally, clusters **1**−**3** are the newest members of a growing family of complexes featuring the H_3L ligand and its deprotonated form. Initially started with the isolation of two $[Cu_4]$, $[Ni_4]$ and $[Co^{III}{}_2Co^{II}{}_3]$ clusters,[5] followed by the characterization of a family of $[Mn^{III}{}_6Ln_2]$ (Ln= Gd, Tb and Dy) and herein with the isolation of **1**−**3**, the ligand and its deprotonated form can adopt three different coordination modes

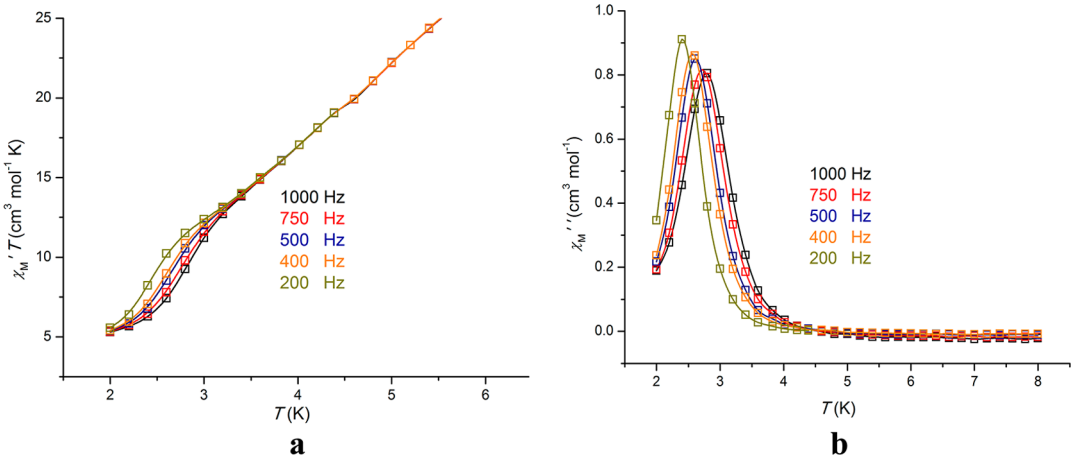

Figure 9. (a) Plot of $\chi_M{}'T$ vs T for complex **2** and (b) plot of $\chi_M{}''$ vs T for complex **2**.

DOI: 10.1021/acs.inorgchem.5b01149
Inorg. Chem. 2015, 54, 7089−7095

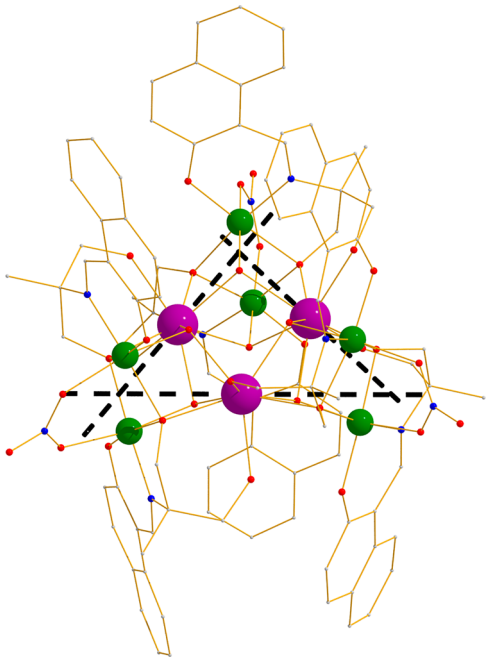

Figure 11. Ground-state magnetic anisotropy axes for the Dy centers present in **2**.

leading to the synthesis of polynuclear complexes with beautiful structures.

Direct Current Magnetic Susceptibility Studies. Variable-temperature dc magnetic susceptibility measurements were performed for all three complexes in the temperature range 5.0–300 K, under an applied field of 0.1 T, and are plotted as $\chi_M T$ vs T in Figure 6. For **1** the room temperature $\chi_M T$ of 32.14 cm^3 K mol^{-1} is very close to the theoretical value of 30.55 cm^3 K mol^{-1} for six non-interacting Ni^{II} ions (g = 2.13) and three non-interacting Gd^{III} ions. Upon cooling, $\chi_M T$ increases to reach the maximum value of 44.80 cm^3 K mol^{-1} at 9 K, before it drops to 7.66 cm^3 K mol^{-1} at 5 K, suggesting the presence of either both ferromagnetic and antiferromagnetic interactions or competing interactions. For complex **2**, the room temperature $\chi_M T$ of 48.50 cm^3 K mol^{-1} is slightly smaller than the theoretical value of 49.42 cm^3 K mol^{-1} for six non-interacting Ni^{II} ions (g = 2.13) and three non-interacting Dy^{III} ions ($S = {}^5/_2$, L = 5, $J = {}^{15}/_2$, $g_j = {}^4/_3$). Upon cooling, the $\chi_M T$ product remains practically unchanged until ~50 K, before it rapidly decreases to the minimum value of 25.89 cm^3 K mol^{-1} at 5 K, suggesting potentially dominant antiferromagnetic interactions; of course, this statement should be met with caution, since the depopulation of the Stark sublevels should clearly affect the shape of the curve. Finally, for **3**, the room temperature $\chi_M T$ of 40.28 cm^3 K mol^{-1} is very close to the theoretical value of 41.35 cm^3 K mol^{-1} for six noninteracting Ni^{II} ions (g = 2.13) and three noninteracting Er^{III} ions ($S = {}^3/_2$, L = 6, $J = {}^{15}/_2$, $g_j = {}^6/_5$). Upon cooling, the $\chi_M T$ value decreases slightly until ~15 K to a value of 38.03 cm^3 K mol^{-1}, before it increases to reach the value of 38.96 cm^3 K mol^{-1} at 5 K. In order to get a qualitative view of the dominant interactions present in each cluster, we performed a Curie–Weiss analysis of the high-temperature (50–300 K) magnetic susceptibility data (Figure 7), yielding θ values of 8.18, 0.74, and −3.03 K for **1**, **2**, and **3**, respectively, albeit this approach cannot exclude the effect of the Stark sublevels' depopulation.

We were able to successfully fit the magnetic susceptibility data for complex **1**, adopting a three-J model (Figure 8) assuming the following interactions: one J_1 interaction between all neighboring Gd–Gd pairs, mediated by two μ_3-OH groups, one J_2 between all neighboring Gd–Ni pairs mediated via two μ_3-O_R alkoxide groups, and one J_3 interaction between neighboring Ni–Ni pairs mediated through two μ_3-O_R alkoxide (Ni–O_R–Ni = 86.1°) and one $\eta^1{:}\eta^1{:}\mu$ nitrate group. Using the powerful program PHI[14] and employing the Hamiltonian eq2

$$\begin{aligned}\hat{H} = &-2J_1(\hat{S}_1\hat{S}_2 + \hat{S}_1\hat{S}_3 + \hat{S}_2\hat{S}_3) - 2J_2(\hat{S}_1\hat{S}_4 + \hat{S}_1\hat{S}_5 + \hat{S}_1\hat{S}_8 \\ &+ \hat{S}_1\hat{S}_9 + \hat{S}_3\hat{S}_4 + \hat{S}_3\hat{S}_5 + \hat{S}_3\hat{S}_7 + \hat{S}_3\hat{S}_6 + \hat{S}_2\hat{S}_6 + \hat{S}_2\hat{S}_7 \\ &+ \hat{S}_2\hat{S}_8 + \hat{S}_2\hat{S}_9) - 2J_3(\hat{S}_4\hat{S}_5 + \hat{S}_6\hat{S}_7 + \hat{S}_8\hat{S}_9) \qquad (2)\end{aligned}$$

afforded J_1 = −0.42 cm^{-1}, J_2 = 0.80 cm^{-1}, and J_3 = 13.13 cm^{-1}, with g_{Ni} = 2.13 and g_{Gd} = 2.00. These parameters lead to the $S = {}^1/_2, {}^3/_2, {}^5/_2, {}^7/_2, {}^9/_2, {}^{11}/_2, {}^{13}/_2, {}^{15}/_2, {}^{17}/_2$, and ${}^{19}/_2$ spin states being populated, even at 2 K, and located within less than 2 cm^{-1}. All J values obtained are in excellent agreement with those reported already in the literature; the exchange interaction between Gd–Gd centers, J_1, should be very weak and either ferromagnetic or antiferromagnetic,[15] J_2 between Ni–Gd should be weak and in many cases have been found to be ferromagnetic,[16] while the interaction Ni–Ni, J_3, should be ferromagnetic according to the magnetostructural correlation reported for $[Ni_4(O_R)_4]$ cubane-like structures, according to which Ni–O_R–Ni angles below 99° should favor ferromagnetic interactions.[17]

Table 1. Ni–Ln SMMs with Fully Formed Out-of-Phase Peaks in the Absence of a Direct Current Field

complex[a]	U_{eff} (K)	τ_0 (s)	ref
$[\{L^1NiLn\}\{W(CN)_8\}]$	15.3	4.5×10^{-7}	18
$[Ni_2Dy_2(L^2)_4(NO_3)_2(DMF)_2]$	18.5	5.4×10^{-7}	19
$[Ni_2Dy_2(L^2)_4(NO_3)_2(MeOH)_2]$	21.3	1.5×10^{-6}	19
$\{[Tb_2Ni_4(L^3)_2Cl_2(OH)_2(CH_3O)_2(CH_3OH)_6]Cl_2(ClO_4)_2$	30	2.09×10^{-9}	20
$\{[Dy_2Ni_4(L^3)_2Cl_2(OH)_2(CH_3O)_2(CH_3OH)_6]Cl_2(ClO_4)_2$	32	10^{-6}–10^{-12}	20
$[Ni(\mu\text{-}L^4)(\mu\text{-}NO_3)Dy(NO_3)_2]$	7.6	7.2×10^{-6}	21
$[\{Dy(hfac)_3\}_2\{Ni(bpca)_2\}]$	4.9	1.3×10^{-6}	22
$[Ni_6Ln_3(OH)_6(LH)_6(NO_3)_3]$	23.8	3.63×10^{-8}	this work
$[Ni_2Dy_3(HL^5)_4]Cl$	85/53.5	5.9×10^{-7} 2.3×10^{-8}	23
$[Ni^{II}_2Ln^{III}_2(CH_3CO_2)_3(HL^6)_4(H_2O)_2](NO_3)_3$	19	4.23×10^{-7}	24

[a] L^1 = Schiff base of 2,2-dimethylpropane-1,3-diamine and 2-hydroxy-3-methoxybenzaldehyde; L^2= Schiff base of *o*-vanillin and 2-aminophenol; L^3 = Schiff base of *o*-vanillin and diethylenetriamine; L^4 = *N*,*N*′,*N*″-trimethyl-*N*,*N*″-bis(2-hydroxy-3-methoxy-5-methylbenzyl)diethylenetriamine; hfac = 1,1,1,5,5,5-hexafluoroacetylacetonate; bpca = bis(2-pyridylcarbonyl)amine anion); L^5 = (*E*)-2,2′-(2-hydroxy-3-((2-hydroxyphenylimino)methyl)-5-methylbenzylazanediyl)diethanol; L^6 = 2-methoxy-6-[(*E*)-2′-hydroxymethyl-phenyliminomethyl]phenolate.

DOI: 10.1021/acs.inorgchem.5b01149
Inorg. Chem. 2015, 54, 7089–7095

Alternating Current Magnetic Susceptibility Studies. For all clusters, ac magnetic susceptibility measurements were performed on polycrystalline samples, in the 1.8−10 K range in zero applied dc field and 3.5 G ac field oscillating at 200−1000 Hz range, as a means of investigating possible SMM behavior. From all three complexes studied, only cluster **2**, $[Ni_6Dy_3]$, displayed interesting behavior; the in-phase, χ_M' (plotted as $\chi_M'T$ vs T, Figure 9a), signal decreases upon decreasing temperature, indicating the presence of low-lying excited states with higher "S" values than the ground-state. Furthermore, it displays frequency-dependent out-of-phase, χ_M'', signals below ∼3.6 K, with fully formed peaks (Figure 9b), thus proving SMM behavior. The ac magnetic susceptibility data were fitted to the Arrhenius relationship (eq 3)

$$\tau = \tau_0 \exp(U_{eff}/kT) \quad (3)$$

where U_{eff} is the effective relaxation barrier, τ is the characteristic relaxation time, τ_0 is the pre-exponential factor, and k is the Boltzmann constant, yielding only one activated regime with U_{eff} = 23.84 K and $\tau_0 = 3.63 \times 10^{-8}$ s (Figure 10).

Furthermore, we were able to calculate the anisotropy axis for each Dy^{III} ion using an electrostatic model recently reported by Chilton et al., based on electrostatic energy minimization for the prediction of the ground-state magnetic anisotropy axis.[26] Following this method and the program MAGELLAN, the ground-state magnetic anisotropy axes in **3** were found to be almost coplanar, "pointing" to the corners of the trigonal prism, and tilted toward the capping nitrate ligands (Figure 11).

Finally, complex **2** joins a small family of Ni−Ln SMMs that contains only a handful of compounds displaying fully formed out-of-phase peaks in the absence of a dc field (Table 1).

CONCLUSIONS

This work expands the use of the triol Schiff base ligand 2-(β-naphthalideneamino)-2-hydroxymethyl-1-propanol, H_3L, in mixed-metal 3d−4f cluster chemistry. Initially employed in 3d chemistry and followed by Mn-4f chemistry, this ligand has now been employed in Ni-4f chemistry, leading to the synthesis and characterization of a family of enneanuclear $[Ni_6Ln]$ clusters (Ln = Gd, Dy and Er), with the Dy analogue displaying SMM behavior with U_{eff} = 24 K. From our work so far concerning the use of the H_3L ligand, we have managed to isolate clusters with nuclearities ranging from four up to nine that display interesting magnetic properties. Further work, as a means of further expanding the cluster chemistry of this ligand in other synthetic schemes, is currently underway.

ASSOCIATED CONTENT

Supporting Information

Crystallographic table and bond distances/angles for complexes **2** and **3** and CIF files for **1**−**3**. The Supporting Information is available free of charge on the ACS Publications website at DOI: 10.1021/acs.inorgchem.5b01149.

AUTHOR INFORMATION

Corresponding Authors

*R.I. E-mail: r.inglis.ed.ac.uk.

*C.J.M. E-mail: komil@chemistry.uoc.gr.

Notes

The authors declare no competing financial interest.

ACKNOWLEDGMENTS

This research has been cofinanced by the European Union (European Social Fund, ESF) and Greek national funds through the Operational Program "Education and Lifelong Learning" of the National Strategic Reference Framework (NSRF) via the THALES Programme (C.J.M. and A.B.C.). R.I. would like to thank The Royal Society of Edinburgh for funding. D.I.T. would like to thank the 89439/2012 Grant of the Aristotle University of Thessaloniki.

REFERENCES

(1) For reviews on SMMs, see the following: (a) Aromi, G.; Brechin, E. K. *Struct. Bonding (Berlin, Ger.)* **2006**, *122*, 1−67. (b) Bircher, R.; Chaboussant, G.; Dobe, C.; Güdel, H. U.; Ochsenbein, S. T.; Sieber, A.; Waldman, O. *Adv. Funct. Mater.* **2006**, *16*, 209−220. (c) Gatteschi, D.; Sessoli, R. *Angew. Chem., Int. Ed.* **2003**, *42*, 268−297. (d) Christou, G.; Gatteschi, D.; Hendrickson, D. N.; Sessoli, R. *MRS Bull.* **2000**, *25*, 66−71. (e) Milios, C. J.; Winpenny, R. E. P. *Struct. Bonding (Berlin)* **2015**, *164*, 1−110. (f) Sorace, L.; Benelli, C.; Gatteschi, D. *Chem. Soc. Rev.* **2011**, *40*, 3092−3104. (g) Wang, X.-Y.; Avendañoa, C.; Dunbar, K. R. *Chem. Soc. Rev.* **2011**, *40*, 3213−3238. (h) Woodruff, D. N.; Winpenny, R. E. P.; Layfield, R. A. *Chem. Rev.* **2013**, *113*, 5110−5148. (i) Langley, S. K.; Le, C.; Ungur, L.; Moubaraki, B.; Abrahams, B. F.; Chibotaru, L. F.; Murray, K. S. *Inorg. Chem.* **2015**, *54*, 3631−3642. (j) Thompson, L. K.; Dawe, L. N. *Coord. Chem. Rev.* **2015**, *289*, 13−31. (k) Demir, S.; Jeon, I.-R.; Long, J. R.; Harris, T. D. *Coord. Chem. Rev.* **2015**, *289*, 149−176. (l) Happ, P.; Plenk, C.; Rentschler, E. *Coord. Chem. Rev.* **2015**, *289*, 238−260. (m) Gómez-Coca, S.; Aravena, D.; Morales, R.; Ruiz, E. *Coord. Chem. Rev.* **2015**, *289*, 379−392. (n) Han, S.-D.; Zhao, J.-P.; Liu, S.-J.; Bu, X.-H. *Coord. Chem. Rev.* **2015**, *289*, 32−48. (o) Craig, G. A.; Murrie, M. *Chem. Soc. Rev.* **2015**, *44*, 2135−2147. (p) Layfield, R. A. *Organometallics* **2014**, *33*, 1084−1099. (q) Piquer, L. R.; Sañudo, E. C. *Dalton Trans.* **2015**, *44*, 8771−8780.

(2) See, for example, the following: (a) Gatteschi, D.; Caneschi, A.; Sessoli, R.; Cornia, A. *Chem. Soc. Rev.* **1996**, *25*, 101−109. (b) Murrie, M. *Chem. Soc. Rev.* **2010**, *39*, 1986−1995. (c) Brechin, E. K. *Chem. Commun.* **2005**, 5141−5153. (d) Lis, T. *Acta Crystallogr.* **1980**, *B36*, 2042−2046. (e) Sessoli, R.; Tsai, H. L.; Schake, A. R.; Wang, S. Y.; Vincent, J. B.; Folting, K.; Gatteschi, D.; Christou, G.; Hendrickson, D. N. *J. Am. Chem. Soc.* **1993**, *115*, 1804−1816. (f) Barra, A. L.; Debrunner, P.; Gatteschi, D.; Schulz, C. E.; Sessoli, R. *Europhys. Lett.* **1996**, *35*, 133−138. (g) Blake, A. J.; Grant, C. M.; Parsons, S.; Rawson, J. M.; Winpenny, R. E. P. *J. Chem. Soc., Chem. Commun.* **1994**, 2363−2364. (h) Yang, E. C.; Hendrickson, D. N.; Wernsdorfer, W.; Nakano, M.; Zakharov, L. N.; Sommer, R. D.; Rheingold, A. L.; Ledezma-Gairaud, M.; Christou, G. *J. Appl. Phys.* **2002**, *91*, 7382−7384. (i) Sun, Z. M.; Grant, C. M.; Castro, S. L.; Hendrickson, D. N.; Christou, G. *Chem. Commun.* **1998**, 721−722.

(3) Ishikawa, N.; Sugita, M.; Ishikawa, T.; Koshihara, S.; Kaizu, Y. *J. Am. Chem. Soc.* **2003**, *125*, 8694−8695.

(4) Lucaccini, E.; Sorace, L.; Perfetti, M.; Costes, J.-P.; Sessoli, R. *Chem. Commun.* **2014**, *50*, 1648−1651.

(5) Canaj, A. B.; Tzimopoulos, D. I.; Philippidis, A.; Kostakis, G. E.; Milios, C. J. *Inorg. Chem.* **2012**, *51*, 10461−10470.

(6) Tziotzi, T. G.; Kalofolias, D. A.; Tzimopoulos, D. I.; Siczek, M.; Lis, T.; Inglis, R.; Milios, C. J. *Dalton Trans.* **2015**, *44*, 6082−6088.

(7) (a) Rao, P. V.; Rao, C. P.; Wegelius, E. K.; Rissanen, K. *J. Chem. Crystallogr.* **2003**, *33*, 39−50. (b) Rao, C. P.; Sreedhara, A.; Rao, P. V.; Verghese, B. M.; Kolehmainen, E.; Lokanath, N. K.; Sridhar, M. A.; Prasad, J. S. *J. Chem. Soc., Dalton Trans.* **1998**, 2383−2394.

(8) Coxall, R. A.; Harris, S. G.; Henderson, D. K.; Parsons, S.; Tasker, P. A.; Winpenny, R. E. P. *J. Chem. Soc., Dalton Trans.* **2000**, 2349−2356.

(9) Llunell, M.; Casanova, D.; Girera, J.; Alemany, P.; Alvarez, S. *SHAPE, version 2.0*, Barcelona, Spain, 2010.

(10) (a) Aronica, C.; Pilet, G.; Chastanet, G.; Wernsdorfer, W.; Jacquot, J. F.; Luneau, D. *Angew. Chem., Int. Ed.* **2006**, *45*, 4659−4662. (b) Aronica, C.; Chastanet, G.; Pilet, G.; Guennic, B. L.; Robert, V.; Wernsdorfer, W.; Luneau, D. *Inorg. Chem.* **2007**, *46*, 6108−6119.

DOI: 10.1021/acs.inorgchem.5b01149
Inorg. Chem. 2015, 54, 7089−7095

(11) Schmidt, S.; Prodius, D.; Mereacre, V.; Kostakis, G. E.; Powell, A. K. *Chem. Commun.* **2013**, *49*, 1696−1698.
(12) Zheng, Y.; Kong, X.-J.; Long, L.-S.; Huang, R.-B.; Zheng, L.-S. *Dalton Trans.* **2011**, *40*, 4035−4037.
(13) Zhuang, G.-L.; Sun, X.-J.; Long, L.-S.; Huang, R. B.; Zheng, L.-S. *Dalton Trans.* **2009**, 4640−4642.
(14) Chilton, N. F.; Anderson, R. P.; Turner, L. D.; Soncini, A.; Murray, K. S. *J. Comput. Chem.* **2013**, *34*, 1164−1175.
(15) See, for example, the following: (a) Black, C. A.; Costa, J. S.; Fu, W. T.; Massera, C.; Roubeau, O.; Teat, S. J.; Aromi, G.; Gamez, P.; Reedijk, J. *Inorg. Chem.* **2009**, *48*, 1062−1068. (b) Rinehart, J. D.; Fang, M.; Evans, W. J.; Long, J. R. *Nat. Chem.* **2011**, *3*, 538−542. (c) Panagiotopoulos, A.; Zafiropoulos, T. F.; Perlepes, S. P.; Bakalbassis, E.; Massonramade, I.; Kahn, O.; Terzis, A.; Raptopoulou, C. P. *Inorg. Chem.* **1995**, *34*, 4918−4920. (d) Roy, L. E.; Hughbanks, T. *J. Am. Chem. Soc.* **2006**, *128*, 568−575.
(16) See, for example, the following: (a) Yukawa, Y.; Aromi, G.; Igarashi, S.; Ribas, J.; Svyagin, S. A.; Krzystek, J. *Angew. Chem., Int. Ed.* **2005**, *44*, 1997−2001. (b) Yamaguchi, T.; Sunatsuki, Y.; Ishida, H.; Kojima, M.; Akashi, H.; Re, N.; Matsumoto, N.; Pochaba, A.; Mrozinski, J. *Bull. Chem. Soc. Jpn.* **2008**, *81*, 598−605. (c) Barta, C. A.; Balyl, S. R.; Read, P. W.; Patrick, B. O.; Thompson, R. C.; Orvig, C. *Inorg. Chem.* **2008**, *47*, 2280−2293. (b) Shiga, T.; Ito, N.; Hidaka, A.; Okama, H.; Kitagawa, S.; Ohba, M. *Inorg. Chem.* **2007**, *46*, 3492−3501. (c) Efthymiou, C. G.; Georgopoulou, A. N.; Papatriantafyllopoulou, C.; Terzis, A.; Raptopoulou, C. P.; Escuer, A.; Perlepes, S. P. *Dalton Trans.* **2010**, *39*, 8603−8605. (d) Georgopoulou, A. N.; Efthymiou, C. G.; Papatriantafyllopoulou, C.; Psycharis, V.; Raptopoulou, C. P.; Manos, M.; Tasiopoulos, A. J.; Escuer, A. *Polyhedron* **2011**, *30*, 2978−2986. (e) Yamaguchi, T.; Sunatsuki, Y.; Ishida, H.; Kojima, M.; Akashi, H.; Re, N.; Matsumoto, N.; Pochaba, A.; Mrozinski, J. *Inorg. Chem.* **2008**, *47*, 5736−5745. (f) Sutter, J.-P.; Dhers, S.; Rajamani, R.; Ramasesha, S.; Costes, J.-P.; Duhayon, C.; Vendier, L. *Inorg. Chem.* **2009**, *48*, 5820−5828. (g) Pasatoiu, T. D.; Sutter, J. P.; Madalan, A. M.; Fellah, F. Z. C.; Duhayon, C.; Andruh, M. *Inorg. Chem.* **2011**, *50*, 5890−5898. (h) Kahn, M. L.; Lecante, P.; Verelst, M.; Mathoniére, C.; Kahn, O. *Chem. Mater.* **2000**, *12*, 3073−3079. (i) Bayly, S. R.; Xu, Z.; Patrick, B. O.; Rettig, S. J.; Pink, M.; Thompson, R. C.; Orvig, C. *Inorg. Chem.* **2003**, *42*, 1576−1583.
(17) Halcrow, M. A.; Sun, J.-S.; Huffman, J. C.; Christou, G. *Inorg. Chem.* **1995**, *34*, 4167−4177.
(18) Sutter, J.-P.; Dhers, S.; Rajamani, R.; Ramasesha, S.; Costes, J.-P.; Duhayon, C.; Vendier, L. *Inorg. Chem.* **2009**, *48*, 5820−5828.
(19) Mondal, K. C.; Kostakis, G. E.; Lan, Y.; Wernsdorfer, W.; Anson, C. E.; Powell, A. K. *Inorg. Chem.* **2011**, *50*, 11604−11611.
(20) Zhao, L.; Wu, J.; Ke, H.; Tang, J. *Inorg. Chem.* **2014**, *53*, 3519−3525.
(21) Colacio, E.; Ruiz-Sanchez, J.; White, F. J.; Brechin, E. K. *Inorg. Chem.* **2011**, *50*, 7268−7273.
(22) Pointillart, E.; Bernot, K.; Sessoli, R.; Gatteschi, D. *Chem.—Eur. J.* **2007**, *13*, 1602−1609.
(23) Chandrasekhar, V.; Bag, P.; Kroener, W.; Gieb, K.; Muller, P. *Inorg. Chem.* **2013**, *52*, 13078−13086.
(24) Ahmed, N.; Das, C.; Vaidya, S.; Langley, S. K.; Murray, K. S.; Shanmugam, M. *Chem.—Eur. J.* **2014**, *20*, 14235−14239.
(25) Sheldrick, G. M. *Acta Crystallogr.* **2008**, *A64*, 112−122.
(26) Chilton, N. F.; Collison, D.; McInnes, E. J. L.; Winpenny, R. E..P.; Soncini, A. *Nat. Commun.* **2013**, *4*, 2551−2557.

DOI: 10.1021/acs.inorgchem.5b01149
Inorg. Chem. 2015, 54, 7089−7095